INTEGRAL MODEL OF A DISCHARGE IN A RAIL ACCELERATOR TAKING INTO ACCOUNT CIRCUMFLUOUS FLOW

S. V. Kukhtetskii, V. A. Lyubochko,
L. P. Mikhailenko, and K. V. Pertsev

UDC 533.9

There is a great deal of interest in MHD setups with a localized discharge: MHD generators with a T layer [1], accelerators with a conduction wave [2], etc. The characteristic feature of these energy converters is the presence of a relatively small conducting region in the flow owing to which the main mass of the comparatively cold nonconducting gas can interact with the external magnetic field. The simplest and in this case most often used model of a discharge is known as the "plasma piston" model [3], which reflects the "ideal" variant of the mechanical interaction of the discharge with the surrounding gas, i.e., the entire gas is raked up by the discharge, as if by a piston. It is evident that the plasma-piston model is a strong idealization, since in many experiments on a rail accelerator [4] at high initial gas pressures ($p_\infty \gtrsim 26$ kPa) the measured value of the velocity of the discharge is significantly higher (by a factor of 1.5-2) than the computed value. Further studies have shown that this could be linked with the partial leakage of gas between the discharge and the lateral walls of the channel, i.e., flow past the discharge. Taking this flow into account substantially complicates the theoretical analysis of the process, since both the form and the characteristic dimensions of the body in the gas flow (discharge) depend strongly on the parameters of the flow. Thus, in this work we studied only one of the simplest integral models of such a discharge, which nevertheless gives good agreement with experiment under our conditions. In the absence of information on the maximum transverse size of the discharge or the thermal wake behind it, this model enables determining the limits within which the main parameters of real setups, such as the velocity of the discharge, the length of the gas plug raked up by the discharge, the efficiency, etc., must lie. In most cases of practical interest these intervals are quite narrow.

The experimental setup consists of a rail accelerator with an external transverse magnetic field. The distance between the electrodes is to be varied 5 cm. The construction of the channel enables its width to be varied in the range 2-5 cm. The working part is 50 cm long. The lateral and end windows enable photographing the discharge simultaneously in several directions for subsequent reconstruction of its form and characteristic dimensions. The average velocity of the discharge and of the shock wave in front of it was measured from signals from a photomultiplier and piezoelectric sensors. Power was supplied to the discharge by rectangular current pulses, formed by a long transmission line. An analogous system supplies power to the winding of Helmholtz coils, creating the external magnetic field in the channel. The rise time of the pulse is $\lesssim 150$ μsec, and the pulse duration is equal to ~ 800 μsec. The discharge current can be varied in the range 10-40 kA and the external magnetic field in the range from 0.3 to 1 T by varying the charging voltage of the long transmission lines. The form of the current pulse and its amplitude were monitored with a Rogowski loop. The investigations were carried out in air, nitrogen, CO_2, and argon. The initial pressure of the working gas in the channel varied from 2.6 to 80 kPa.

We shall examine some experimental results of a phenomenological character. Figure 1 shows a typical series of photographs of the discharge for three working gases: a) CO_2, b) nitrogen, and c) argon. The discharge current I = 20 kA, the external magnetic field B = 0.6 T, and the initial gas pressure in the channel $p_\infty = 26$ kPa. The exposure time of each frame is equal to 3 μsec, and the time interval between the frames is equal to 12 μsec. The distance between the vertical reference lines is equal to 5 cm. The discharge current and the external magnetic field rise up to their stationary values indicated above during the initial period ($t \lesssim 100$-150 μsec). At the same time a localized current-carrying region is formed and accelerated. Then the discharge begins to move with a practically constant velocity, on the whole retaining its geometry and characteristic dimensions. An exception is the

Krasnoyarsk. Translated from Zhurnal Prikladnoi Mekhaniki i Tekhnicheskoi Fiziki, No. 1, pp. 40-46, January-February, 1986. Original article submitted November 10, 1984.

0021-8944/86/2701-0035$12.50

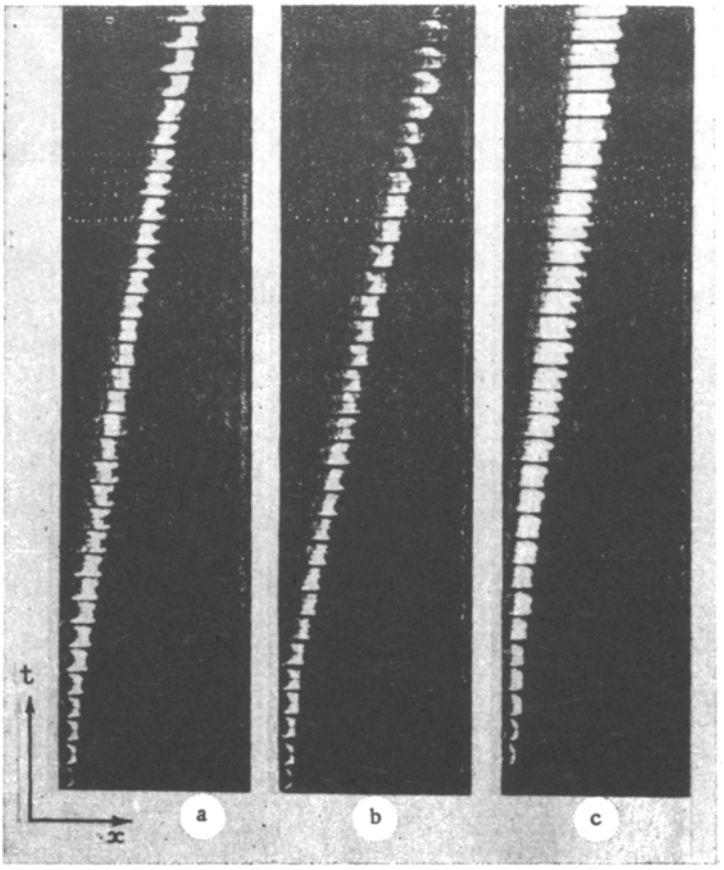

Fig. 1

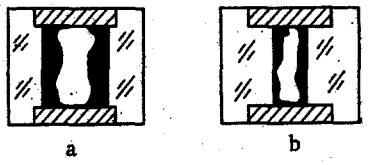

Fig. 2

discharge in argon (Fig. 1c), which continues to expand along the channel throughout the entire process. In this case, the velocity of the discharge is understood to mean the average velocity of its leading edge.

The dynamics of the discharge in the transverse direction was not studied in detail, but we must make one remark which is important for what follows. The transverse cross section of the core of the discharge A_d reaches its stationary value 150-200 μsec after the discharge is initiated and constitutes, as a rule, not more than 40-60% of the transverse cross section of the channel A_0. Two typical photographs of the discharge from the end are shown in Fig. 2; the channel is 4 (a) and 2.1 (b) cm wide. In both cases the working gas is argon, p_∞ = 26 kPa, IBh/A_0p_∞ = 17 (h = 5 cm is the height of the channel), and the ratios A_d/A_0 practically coincide (for the given conditions $A_p/A_0 \approx 0.56$). The stationary transverse size is reached by two methods. For a low current growth rate ($\lesssim 10^8$ A/sec) and small energy input into preionization, the discharge, expanding gradually, reaches its stationary transverse size within 100-150 μsec. In the case of rapid current growth at first the entire transverse cross section of the channel is filled (within 50-100 μsec), and then the discharge begins to narrow until it reaches (after 50-150 μsec) the same transverse cross section as in the first case (for equal stationary values of the remaining parameters).

Although the characteristic dimensions and the average velocity of the discharge remain virtually constant after the transient process, the internal structure and form of the current-carrying region are substantially nonstationary. This is especially clearly seen in discharges in nitrogen and air, where the separation of the discharge into several isolated

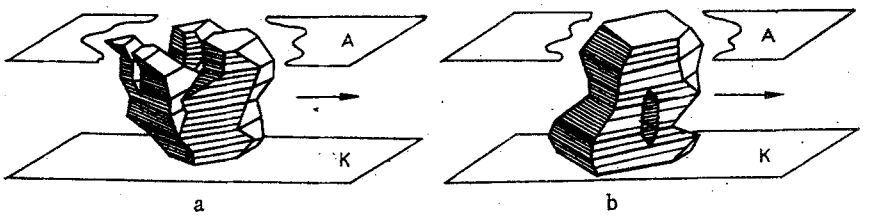

Fig. 3

current-carrying channels or their complete destruction as a local formation is sometimes observed. In the last case the current is distributed over almost the entire interelectrode gap of the accelerator. Figure 3 shows schematically two configurations of the discharge in nitrogen (I = 20 kA, B = 0.6 T, p_∞ = 26 kPa), reconstructed from simultaneous photographs from three aspects. The physical factors responsible for the irregularity of the internal structure of the discharge and its destruction are still not completely understood, so that in this work we shall confine our attention to the quasistationary motion of the discharge, as, for example, in Fig. 1. In argon such configurations are realized under almost all conditions studied, in CO_2 they appear in 80 to 90% of the cases, while in nitrogen and air they appear in 30-40% of the cases.

Since the purpose of this work is to establish the integral characteristics of the accelerator, it makes sense to forego a multidimensional description of the gas flow near the discharge and to confine our attention to the stationary quasi-one-dimensional case. We shall transform to a reference system fixed to the discharge. Then the flow of gas outside the discharge can be viewed as a flow in a pipe with a variable cross section $A(x) = A_0 - A_d(x)$, where where A_0 is the transverse cross section of the channel and $A_d(x)$ is the transverse cross section of the current-carrying region (core of the discharge).

Let us estimate the thickness of the viscous boundary layer in the discharge. Reynolds number $Re = u^*l/\nu \gtrsim 10^5$, where $u^* \sim 500$ m/sec is the characteristic velocity of the gas flowing past the discharge, $l \sim 5$ cm is the length of the discharge, and ν is the kinematic viscosity. From here $\delta \sim 0.37(Re)^{-1/5} l \lesssim 0.2$ cm [5], which is much less than the characteristic thickness of the gap between the discharge and the lateral walls of the channel [$(A_0 - A_d)/h \sim 1$-2 cm]. The friction forces, caused by the tangential stresses at the discharge boundary, are also weak. Indeed, viewing the discharge as a flat plate, the friction force can be estimated using the formula in [5] $F_{fr} \sim \rho u^{*2} l h c_f/2 \sim 1$-2 N, which is negligibly small compared with Ampere's force, applied to the discharge, $F_m \sim IBh \sim 10^3$ N. Thus the pressure resistance force, i.e., the resultant gasdynamic pressure p on the surface of the discharge, plays the main role in the force balance, and the viscous effects can be neglected in this problem.

The thermal layer and the thermal wake behind the discharge can significantly affect the dynamics of the discharge, since because of the radiant heat transfer their thickness can be much larger than the thickness of the viscous boundary layer and comparable to the cross section of the channel. By thermal layer here we mean the layer of gas between the core of the discharge and the external flow, heated up to a temperature of $(5\text{-}6)\cdot 10^3$ °K, the current density in which is still too small to affect significantly its dynamics. We shall assume that the velocity of the gas in the thermal layer and in the thermal wake coincide with the velocity of the external flow, while their effect on the flow is expressed, first, as a partial displacement of the cold gas out of the discharge toward the lateral walls, which in the quasi-one-dimensional approximation corresponds to decreasing the effective cross section of the gap between the discharge and the lateral walls of the channel and also the cross section of the channel behind the discharge, and second, unlike the external cold gas behind the discharge, the velocity of the gas in the thermal wake is subsonic, as a result of which the presence of the back end wall of the channel becomes significant.†

We shall now study the scheme of the flow (Fig. 4). The supersonic gas flow is incident on the core of the discharge 5. At the same time, a shock wave 1 moves upstream. The subsonic flow behind the shock-wave front begins to accelerate in the converging gap between the discharge and the lateral walls of the channel, until it reaches sonic velocity in the critical section A*. The flow then expands up to the cross section A_1, but now with a supersonic velocity. The transition through the sonic velocity is necessary here, since in this case

†We have in mind the velocity in the reference system fixed to the discharge.

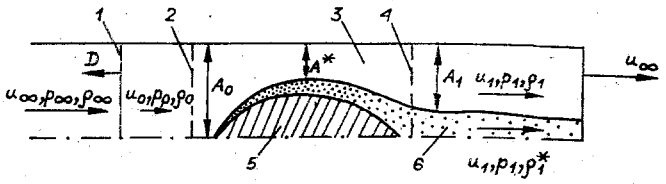

Fig. 4

gas can be accumulated and an outgoing shock wave formed only in front of the discharge, which always occurred in the experiment. Let us assume that the part of the incident gas flow which forms the thermal wake 6 is much smaller than the full flow $\rho_0 u_0$ of the gas flowing past the discharge. This proposition is valid, at least, for molecular gases. Estimates show that even if all Joule heating in the discharge goes into heating and dissociation of the gas flowing past the discharge, in this case only a small part of the gas (not more than 10%) is heated up to $(5\text{-}6)\cdot 10^3$ °K. Let us assume also that after the critical section A* the gas expands in an equilibrium manner, i.e., the flow in region 3 is isentropic.

The parameters of the flow entering into the problem are indicated in Fig. 4, where ρ_∞, p_∞, u_∞, ρ_0, p_0, u_0, ρ_1, p_1, u_1 are the density, pressure, and velocity, respectively, of the unperturbed gas, of the shock-heated gas in front of the discharge, and of the gas behind the discharge; ρ_1^* is the density of the gas in the thermal wake; and D is the outgoing velocity of the shock wave in the reference system fixed to the discharge. We seek the stationary solution. In this case Ampere's force IBh must be equal to the force of resistance of the discharge. Applying the momentum theorem [5] to the control surfaces 2 and 4 (see Fig. 4), we have

$$IBh = \rho_0 u_0^2 A_0 + p_0 A_0 - \left[\rho_1 u_1^2 A_1 + \rho_1^* u_1^2 (A_0 - A_1) + p_1 A_0\right] = A_0\left\{p_0 - p_1 + \rho_0 u_0^2 - \rho_1 u_1^2\left[\frac{A_1}{A_0} + \frac{\rho_1^*}{\rho_1}\left(1 - \frac{A_1}{A_0}\right)\right]\right\}. \quad (1)$$

Substituting into (1) the equation of continuity

$$\rho_0 u_0 A_0 = \rho_1 u_1 A_0\left[\frac{A_1}{A_0} + \frac{\rho_1^*}{\rho_1}\left(1 - \frac{A_1}{A_0}\right)\right], \quad (2)$$

we obtain

$$\frac{IBh}{A_0 p_0} = 1 - \frac{p_1}{p_0} - \frac{\rho_0 u_0^2}{p_0}\left(\frac{u_1}{u_0} - 1\right) = 1 - \frac{p_1}{p_0} - \gamma M_0^2\left(\frac{M_1}{M_0}\frac{c_1}{c_0} - 1\right), \quad (3)$$

where $c = \sqrt{\gamma p/\rho}$ is the velocity of sound, $M = u/c$ is Mach's number, and γ is the adiabatic index. Using the well-known relations for isentropic flow in channels with a variable cross section [6]

$$\left(\frac{A_1}{A_0}\right)^2 = \frac{M_0^2}{M_1^2}\left(\frac{1 + \frac{\gamma-1}{2}M_1^2}{1 + \frac{\gamma-1}{2}M_0^2}\right)^{\frac{\gamma+1}{\gamma-1}}, \quad \frac{p_1}{p_0} = \left(\frac{1 + \frac{\gamma-1}{2}M_0^2}{1 + \frac{\gamma-1}{2}M_1^2}\right)^{\frac{\gamma}{\gamma-1}}. \quad (4)$$

M_1 and M_0 can be expressed in terms of A_1/A_0 and p_1/p_0:

$$M_1 = M_0\left(\frac{p_1}{p_0}\right)^{-\frac{\gamma+1}{2\gamma}}\left(\frac{A_1}{A_0}\right)^{-1}, \quad M_0^2 = \frac{2}{\gamma-1}\frac{1 - \left(\frac{p_1}{p_0}\right)^{\frac{\gamma-1}{\gamma}}}{\left(\frac{p_1}{p_0}\right)^{-\frac{2}{\gamma}}\left(\frac{A_1}{A_0}\right)^{-2} - 1}. \quad (5)$$

Substituting these expressions into (3) and using the relations

$$\frac{\rho_1}{\rho_2} = \left(\frac{p_1}{p_0}\right)^{\frac{1}{\gamma}}, \quad \frac{c_1}{c_0} = \left(\frac{p_1}{p_0}\right)^{\frac{\gamma-1}{2\gamma}} \quad (6)$$

we find for the isentropic flow an expression for the pressure p_0 in the shock-heated gas plug:

$$\frac{p_0}{p_\infty} = \frac{\frac{IBh}{A_0 p_\infty}}{1 - \frac{p_1}{p_0} - \frac{2\gamma}{\gamma - 1}\frac{A_1}{A_0}\left(\frac{p_1}{p_0}\right)^{\frac{1}{\gamma}} \frac{1 - \left(\frac{p_1}{p_0}\right)^{\frac{\gamma-1}{\gamma}}}{1 + \frac{A_1}{A_0}\left(\frac{p_1}{p_0}\right)^{\frac{1}{\gamma}}}}. \tag{7}$$

We obtain a second equation relating p_0/p_∞ and p_1/p_0 as follows. The conditions of conservation of mass and momentum on the front of the shock wave have the form

$$\rho_\infty(u_\infty + D) = \rho_0(u_0 + D),\ p_\infty + \rho_\infty(u_\infty + D)^2 = p_0 + \rho_0(u_0 + D)^2. \tag{8}$$

Eliminating D from these equations, we write

$$u_\infty - u_0 = c_\infty \left[\frac{\left(\frac{p_0}{p_\infty} - 1\right)\left(\frac{\rho_0}{\rho_\infty} - 1\right)}{\gamma\frac{\rho_0}{\rho_\infty}}\right]^{1/2}. \tag{9}$$

Substituting into (9) the equation of the Hugoniot adiabat

$$\frac{\rho_0}{\rho_\infty} = \frac{\frac{\gamma+1}{\gamma-1}\frac{p_0}{p_\infty} + 1}{\frac{p_0}{p_\infty} + \frac{\gamma+1}{\gamma-1}},$$

we have

$$u_\infty - u_0 = c_\infty \frac{\frac{p_0}{p_\infty} - 1}{\left[\frac{\gamma(\gamma-1)}{2}\left(\frac{\gamma+1}{\gamma-1}\frac{p_0}{p_\infty} + 1\right)\right]^{1/2}}. \tag{10}$$

The velocity u_∞ can be related to the velocity of the gas behind the discharge u_1 and, therefore, to p_1 by two methods: by introducing together with A_1/A_0 one other parameter $1 - A^*/A_0$, characterizing the critical cross section of the discharge, or, taking into account the subsonic nature of the flow in the thermal wake [$c^* \sim (2\text{-}2.5)\cdot 10^3$ m/sec, $u_\infty \sim u_1 \sim (1\text{-}1.5)\cdot 10^3$ m/sec], by using the boundary condition $u_\infty = u_1$ directly behind the discharge, i.e., the velocity of the gas behind the discharge u_1 coincides with the velocity of the back end wall u_∞. The second method is preferable physically, since the discharge, not being a solid body, most likely adjusts itself so that the flow satisfies the required boundary conditions. This phenomenon has at the present time not been completely studied. In this work we assume that the following condition holds:

$$u_\infty = u_1. \tag{11}$$

Using the relations (5), (6), and the boundary condition (11), we obtain from (10) a second equation relating p_0/p_∞ and p_1/p_0:

$$\frac{\left[1 - \left(\frac{p_1}{p_0}\right)^{\frac{\gamma-1}{\gamma}}\right]\left[1 - \left(\frac{p_1}{p_0}\right)^{\frac{1}{\gamma}}\frac{A_1}{A_0}\right]}{1 + \left(\frac{p_1}{p_0}\right)^{\frac{1}{\gamma}}\frac{A_1}{A_0}} = \frac{\left(\frac{p_0}{p_\infty} - 1\right)^2}{\gamma\frac{p_0}{p_\infty}\left(\frac{p_0}{p_\infty} + \frac{\gamma+1}{\gamma-1}\right)}. \tag{12}$$

Solving the system (7) and (12) we can find p_1/p_0 and p_0/p_∞, and then M_0 from (5) and $M_\infty = u_\infty/c_\infty$, coinciding in the laboratory coordinate system with the relative velocity of the discharge, from (10). The solution depends on two dimensionless parameters: IBh/A_0p_∞ and A_1/A_0. The first parameter is easily monitored in the experiment, while the value of the second parameter depends on many factors, such as the length of the discharge along the channel, the radiant heat conduction, the type of gas, the degree of turbulent mixing of the thermal layer both with the discharge and with the gas flowing past the discharge, etc.

Figure 5 shows the dependence of the velocity of the discharge M_∞ on IBh/A_0p_∞ for the four gases studied: CO_2 (a), nitrogen and air (b), and argon (c). The curves 1 correspond to

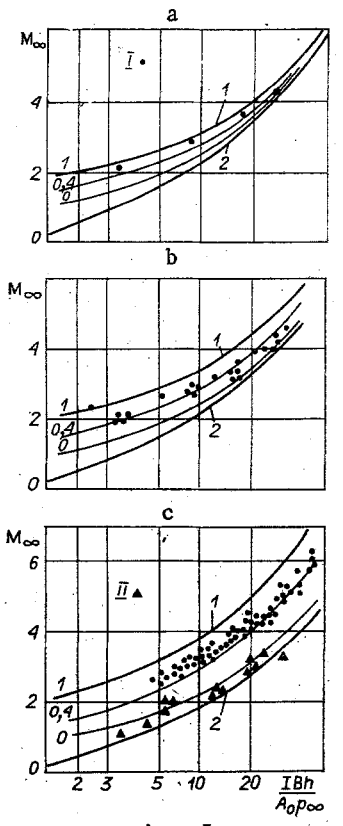

Fig. 5

a negligibly small thermal wake ($A_1/A_0 \to 1$), i.e., an actually pure isentropic flow past the core of the discharge, while the curves 2 correspond to the plasma-piston model ($M_0 = 0$). It is easy to show that taking into account the factors neglected in this work, such as the nonequilibrium nature of the state, the viscous friction, the possible turbulence of the flow in region 3 (see Fig. 4), will yield values of M_∞ lying between the curves 1 and 2 in Fig. 5. It is evident from the graphs that as γ decreases and $IBh/A_0 p_\infty$ increases, the curves 1 and 2 converge to one another, i.e., for polyatomic molecular gases with $IBh/A_0 p_\infty \gtrsim 10$ the physically admissible solutions almost coincide with the plasma-piston model (under the condition, of course, that the characteristic size of the discharge is of the order of the transverse size of the channel). The same graphs show the experimentally determined values of the discharge velocity under different conditions, indicated at the beginning of this work. The relatively high heat capacity of CO_2 leads to the fact that the thickness of the thermal wake becomes small, and as a result of this the experimental points fall almost on the curve 1 (Fig. 5a). For nitrogen and air, as the discharge current I increases, the discharge became longer along the channel, increasing hardly at all in the transverse section. The thickness of the thermal wake in this case should increase. This gives rise to the fact that as $IBh/A_0 p_\infty$ increases the experimental points approach the curve 2 (Fig. 5b). This effect is observed especially clearly in argon (Fig. 5c) because of its relatively low specific heat capacity at the temperatures $(4-6)\cdot 10^3$ °K. The points I correspond to relatively weak discharge currents I and high values of the external magnetic field, while the points II correspond to the opposite case. In the first case a discharge of the order of 3-5 cm long was established, while in the second case the discharge was 10-15 cm long. It is evident that with a long discharge the experimental points lie almost on the curve 2 (Fig. 5c). The transverse cross section of the core of the discharge does not exceed 60% of the cross section of the channel. The photograph in Fig. 2 refers precisely to this case.

In conclusion we note the following.

1. Under the conditions studied the core of the discharge sometimes does not fill the transverse cross section of the channel completely (with the exception of the initial stage with the rapid current growth), so that the gas flow past the discharge and the partial heating of the flowing gas become important.

2. In analyzing the efficiency or the overall working capacity of MHD converters with a localized discharge, for the worst (in the mechanical sense) variant the model corresponding to isentropic flow past the discharge with negligibly small thermal wake ($A_1/A_0 \to 1$) can be studied. In this case it is assumed that the size of the discharge is comparable to the transverse size of the channel. The best variant is the plasma-piston model. In the case of a polyatomic molecular gas (in particular, CO_2) for $IBh/A_0p_\infty \gtrsim 10$-15 both models are virtually identical.

3. The comparison of the experimental and computed values of the velocities of the discharge in the "railtron" made above shows that the experimental points fall into the indicated interval, approaching one or another limiting case depending on the conditions and type of gas.

We thank V. S. Sokolov, O. G. Parfenov, V. S. Slavin, and A. D. Lebedev for useful discussions and remarks in the course of this work.

LITERATURE CITED

1. V. A. Derevyanko, V. S. Slavin, and V. S. Sokolov, "Magnetohydrodynamic electricity generator based on the products of gasification of lignite," Zh. Prikl. Mekh. Tekh. Fiz., No. 5 (1980).
2. B. W. Boreham, "Study of traveling conduction wave accelerator," AIAA J., 14, No. 1 (1976).
3. S. A. Belyaev, D. A. Gol'dina, et al., "Calculation of the nonstationary acceleration of plasma in the uniform approximation," Preprint of the Institute of Applied Mathematics of the USSR Academy of Sciences, No. 53 (1969).
4. S. V. Kukhtetskii, V. A. Lyubochko, and A. D. Lebedev, "Some features of the motion of a strong-current quasistationary discharge in a magnetic field," in: Abstracts of Reports at the 9th All-Union Conference on Low-Temperature Plasma Generators [in Russian], Ilim, Frunze (1983).
5. G. Shlikhting, Boundary-Layer Theory [in Russian], Nauka, Moscow (1974).
6. L. G. Loitsyanskii, Mechanics of Liquids and Gases [in Russian], Nauka, Moscow (1970).

DYNAMICS OF LIQUID FILMS. PLANE FILMS WITH FREE RIMS

V. M. Entov, A. N. Rozhkov,
U. F. Feizkhanov, and A. L. Yarin

UDC 532.522+532.62+532.135

The discharge of a liquid from thin slits of finite length ("slit nozzles or dies") results in the formation of characteristic V-shaped plane streams (free dynamic films) which are bounded by free "rims" — boundary streams [1] (Fig. 1a). A similar flow is realized in purer form if a small section is cut out from the dynamic film created, for example, in the flow of a stream against a barrier. Here, the section is isolated by placing two thin blades or wires in the path of the liquid [2]. It is clear that the form of the film and the velocity field in it contain information on the stress field, and quantitative analysis of such flows may be a means of studying the rheology of the liquid. Along with this, it is important to analyze flow in films and in the free rims at their edges to understand the conditions of fragmentation and atomization of the liquid. Presented below are results of theoretical and experimental studies of free films with boundary streams for ideal and viscoelastic liquids.

1. Formulation of the Problem. Taking advantage of the thinness of the film and boundary stream, we can describe the flow as a combination of two-dimensional equations in the region G occupied by the film and one-dimensional "stream" equations on the axis S of the boundary stream. The boundary stream is distinguished from the rest of the liquid by the fact that mass and momentum exchange occur on the lateral surface of the stream. The motion of liquid in the film and rim is conveniently described in polar coordinates (r, θ) in the middle plane of the film. We will examine small segments ABB'A' of a free rim on the edge

Moscow. Translated from Zhurnal Prikladnoi Mekhaniki i Tekhnicheskoi Fiziki, No. 1, pp. 47-53, January-February, 1986. Original article submitted October 10, 1984.

